

Heat perturbations spreading in the Fermi-Pasta-Ulam- β system with next-nearest-neighbor coupling: Competition between phonon dispersion and nonlinearity

Daxing Xiong*

Department of Physics, Fuzhou University, Fuzhou 350108, Fujian, China

We employ the heat perturbations correlation function to study thermal transport in the one-dimensional (1D) Fermi-Pasta-Ulam- β lattice with both nearest-neighbor and next-nearest-neighbor couplings. We find that such a system bears a peculiar phonon dispersion relation, and thus there exists a competition between phonon dispersion and nonlinearity that can strongly affect the heat correlation function's shape and scaling property. Specifically, for small and large anharmonicity, the scaling laws are ballistic and superdiffusive types, respectively, which are in good agreement with the recent theoretical predictions; whereas in the intermediate range of the nonlinearity, we observe an unusual multiscaling property characterized by a *nonmonotonic* delocalization process of the central peak of the heat correlation function. To understand this multiscaling laws, we also examine the momentum perturbations correlation function and find a transition process with the same turning point of the anharmonicity as that shown in the heat correlation function. This suggests coupling between the momentum transport and the heat transport, in agreement with the theoretical arguments of mode cascade theory.

I. INTRODUCTION

Despite decades of research, our understanding of anomalous heat transport in one-dimensional (1D) momentum-conserving systems is still scarce [1–3]. There are various theoretical models and three main numerical approaches which devote to solving this issue. The theoretical techniques include the mode coupling theory [4, 5], the renormalization group method [6], the mode cascade assumption [7–10], the phenomenological Lévy walks model [11, 12], and the nonlinear fluctuating hydrodynamics theory [13, 14], etc. The early two numerical approaches are based on either the direct nonequilibrium molecular dynamics simulations [15–19] or the Green-Kubo formula [20–22]. In the former, the ends of the system are first connected to heat baths with a small temperature difference for a long time. After a steady state has been obtained, one then observes the heat current flowing across the system, and finally derives the thermal conductivity. In the latter, one usually examines the long time asymptotic behavior of the heat current autocorrelation function (or power spectra), and then use Green-Kubo formula to get the heat conductivity. In this respect, the first three theoretical models [4–10] are just devoted to prediction of the time scaling behavior of the heat current autocorrelation function. In particular, the mode cascade theory suggested for the first time that one should take the coupling between the momentum transport and the heat transport into account, and demonstrated that due to this coupling, to obtain an accurate prediction, the heat current power spectra at sufficiently low frequencies should be probed [7–10].

The third numerical approach is based on the pertur-

bations correlation functions. This is inspired by the idea of diffusion of energy in the lattice systems. As is well known, in such many-body systems, particles are mainly located around their equilibrium positions. So there is no sense to talk about the diffusion of energy of the associated particles. While the collective system dynamics creates a “tissue”, which can react to small local perturbations affecting its dynamics. Eventually, the propagation of perturbations defines the overall information of transport [11, 23–26].

With such an idea in mind, understanding the energy and heat transport processes via their perturbations correlation functions is a relevant fascinating topic of theoretical research [11–14, 27–37]. The early numerical works indicated that for general 1D nonlinear nonintegrable momentum-conserving systems, a quasi superdiffusive Lévy walks profile of the energy perturbations correlation function can be always observed [12, 27–29], which is the evidence of anomalous heat transport. Viewing this fact, such superdiffusive transport has been subsequently understood from the single particle's Lévy walks model in the superdiffusive regime after considering the particle's velocity fluctuations [11, 12], although the connection between them is only phenomenological [11]. Later, a more detailed mechanism has been considered in a broad context of hydrodynamics [13, 14], where the authors developed a nonlinear version of the hydrodynamics theory and explained the observed Lévy walks profile as a combination of the heat and sound modes' correlations [13, 14, 29]. The main achievement of this hydrodynamics theory is that it can be used to predict the scaling property of the heat and momentum perturbations spreading correlation functions in certain nonlinear systems and thus is greatly helpful to our understanding of anomalous heat transport [30]. This is because the heat and the sound modes' correlations are usually conjectured to correspond to the heat and the

*Electronic address: phyxiongdx@fzu.edu.cn

momentum perturbations correlation functions, respectively [29]. In particular, for generic systems of nonzero pressure, such as the Fermi-Pasta-Ulam- α - β (FPU- α - β) model with asymmetric (odd) interparticle potential, the prediction for the sound modes' correlation is Kardar-Parisi-Zhang (KPZ) scaling [38]; while for the particular FPU- β system with symmetric (even) interparticle potential, it is not KPZ but Gaussian scaling [13, 29]. This is consistent with the argument that the momentum current power spectrum does (does not) diverge at low frequency for systems with odd (even) interparticle potential [4, 7–10].

In spite of these achievements, an unclear point from the nonlinear hydrodynamics theory may be that, we still don't know to what extent of the strength of the nonlinearity it would be applicable. Since the theory aims to deal with the nonlinear systems, it requires the system's dynamics to be sufficiently chaotic so as to have good mixing in time [14]. So it is quite possible that, for certain linear integrable systems, the nonlinear hydrodynamics theory is not valid any more [34]. As to the latter systems, a recent concept called “phonon random walks” might be worthwhile [39], based on which the linear system's ballistic heat perturbations spreading correlation function can be instead understood by a quantum-like wave function's modulus square, where the different systems' distinct phonon dispersion relations are a key factor. In addition, in this theory the momentum perturbations correlation function is proved to be the corresponding wave function's real part [39].

Combining the above reviewing progress, one may recognize that the coupling between the heat transport and the momentum transport should naturally exist and this coupling will be exhibited quite differently in various systems. This then leads to the fact that different theoretical models would be applicable to different systems or to the same system under different strength of the nonlinearity. In particular, for the strongly nonlinear systems where the effects of nonlinearity dominate, the nonlinear hydrodynamics theory [13, 14] could present some universal predictions; while as to the linear systems without including the nonlinearity, the phonon dispersion relation now plays a major role [39] and there is not mode and mode's coupling [40]. Therefore, to provide a complete picture of thermal transport, such as the normal, ballistic, superdiffusive types, and to understand the coupling between the heat transport and the momentum transport in different situations, both the effects of nonlinearity and phonon dispersion relation are crucial and necessary to take into account. Motivated by this and in view of that almost all of above literatures only focused on the systems with nearest-neighbor (NN) interaction, we here consider a 1D FPU- β system with both the NN and next-nearest-neighbor (NNN) interactions. The advantage of this system is that it bears a peculiar phonon dispersion relation. With this advantage, we then can adjust the strength of the nonlinearity to see how such particular phonon dispersion relation could together with the non-

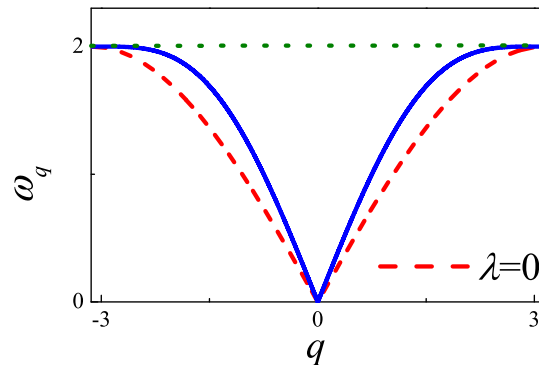


FIG. 1: The phonon dispersion relation for the FPU- β chain with both NNN and NN couplings ($\lambda = 0.25$), which is compared to the counterpart harmonic chain of $\lambda = 0$ (dashed line). The horizontal dotted line indicates $\omega_q = 2$ near the Brillouin zone boundary.

linearity affect the system's heat transport and its scaling property. Such a research strategy will also help us to reveal the detailed coupling between the heat transport and the momentum transport in this particular system, which may provide insights into further developing a theory to bridge our present understanding of linear and nonlinear systems' thermal transport, after combining both factors of phonon dispersion relation and nonlinearity.

The rest of this paper is structured in the following way: In Sec. II we introduce the reference model and emphasize its peculiar phonon dispersion relation. Sec. III describes the simulation method to derive the corresponding perturbations correlation functions. In Sec. IV we present our main results, and Sec. V is devoted to discussion of the mechanism. Finally we close with a summary in Sec. VI.

II. MODEL

As mentioned, in what follows we focus on a 1D FPU- β lattice with both NN and NNN interactions [41]. Such a system's Hamiltonian is

$$H = \sum_{k=1}^L \left[\frac{p_k^2}{2} + V(r_{k+1} - r_k) + \lambda V(r_{k+2} - r_k) \right] \quad (1)$$

with r_k the displacement of the k th particle from its equilibrium position and p_k its momentum. The potential takes the FPU- β type of $V(\xi) = \xi^2/2 + \beta\xi^4/4$ with β to be adjustable and representing the nonlinearity. The parameter λ controls the comparative strength of the NNN coupling to the NN coupling and if it is fixed at $\lambda = 0.25$ reproducing a special phonon dispersion relation (under harmonic approximation):

$$\omega_q = \sqrt{4 \sin^2(q/2) + \sin^2(q)} \quad (2)$$

as shown in Fig. 1. Here q is the wave number and ω_q is the corresponding frequency. From Fig. 1 we know

that such a phonon dispersion relation has a main feature, i.e., the group velocity $v_g = d\omega_q/dq$ is very close to zero in a wider q domain near the Brillouin zone boundary. This unusual property can favor the formation of a special highly localized excitation [intradband discrete breathers (DBs)] [42] in the presence of appropriate nonlinearity and thus is conjectured to greatly influence thermal transport [41]. In addition, we note that some recent works have indicated that the FPU- β lattice including such kind of long range interactions beyond the NN couplings can lead to some unusual effects on thermal transport [43] and thermal rectification [44]. All of these understanding are also the motivations that we choose to study such a system.

III. METHOD

We shall employ the equilibrium fluctuation-correlation method [27, 29] to investigate the propagation of heat perturbations. This approach has been first proposed by Zhao [27] for studying the site-site total energy fluctuations spreading and then extended to be applicable to investigate the space-space fluctuations spreading [29]. For further detailed implementation, one can also refer to [45]. Due to the apparent advantage of avoiding the emerging statistical fluctuations [11, 12], such popular efficient simulation method has been widely used in many publications [12, 28, 31–33, 35–37].

To make a comparison with the prediction of hydrodynamics theory [13, 14], we shall focus on the following two space-space correlation functions of the heat perturbations and momentum perturbations [29], i.e.,

$$\rho_Q(m, t) = \frac{\langle \Delta Q_j(t) \Delta Q_i(0) \rangle}{\langle \Delta Q_i(0) \Delta Q_i(0) \rangle} \quad (3)$$

and

$$\rho_p(m, t) = \frac{\langle \Delta p_j(t) \Delta p_i(0) \rangle}{\langle \Delta p_i(0) \Delta p_i(0) \rangle}, \quad (4)$$

respectively. Here $m = j - i$; $\langle \cdot \rangle$ denotes the spatiotemporal average. To describe the space-space correlation, one can divide the 1D lattice into several equivalent bins and thus, i and j are the labels of the bins. In practice, we will set the averaged number of particles in each bin to be $N_i = (L - 1)/b$ with b the total number of the bins. Under such space description, $\Delta Q_i(t) \equiv Q_i(t) - \langle Q_i \rangle$ and $\Delta p_i(t) \equiv p_i(t) - \langle p_i \rangle$ then define the heat perturbations and momentum perturbations in the i th bin at time t , respectively, with $Q_i(t)$ and $p_i(t)$ the corresponding heat energy and momentum densities. $p_i(t)$ is readily to calculate, one just needs to sum the related single particle's momentum $p_k(t)$ within the bin, namely $p_i(t) \equiv \sum_k p_k(t)$. To compute $Q_i(t)$, we employ the definition of $Q_i(t) \equiv E_i(t) - \frac{\langle (E) + \langle F \rangle M_i(t) \rangle}{\langle M \rangle}$ [46, 47] from thermodynamics, where $E_i(t) \equiv \sum_k E_k(t)$, $M_i(t) \equiv \sum_k M_k(t)$,

and $F_i(t) \equiv \sum_k F_k(t)$ are the total energy, number of particles and internal pressure in that bin, respectively, with $E_k(t)$, $M_k(t)$, $F_k(t)$ the corresponding single particle's energy, density, and pressure. From the perspective of hydrodynamics theory, $\rho_Q(m, t)$ and $\rho_p(m, t)$ might represent the heat mode's and sound modes' correlations, respectively [13, 14, 29], based on which one might be able to construct the corresponding energy and particle perturbations correlation functions [29]. Therefore, our following study of $\rho_Q(m, t)$ and $\rho_p(m, t)$ is also partially motivated by this connection.

The simulations of both correlation functions are performed as follows: Initially we contact the system with a Langevin heat bath [1, 2] of temperature $T = 0.5$ (fixed throughout the paper) to get a equilibrium state. Then after this thermalized equilibrium state has been prepared, we utilize the Runge-Kutta integration algorithm of seventh to eighth order with a time step $h = 0.05$ to evolve the system. During such evolution, we then sample the relevant data and calculate the corresponding correlation functions.

To perform the simulations, we apply the following settings: periodic boundary conditions with a size of $L = 4001 - 6001$ is adopted, which will allow a perturbation of heat and momentum located at the center of the chain to spread out a long time up to $t = 900$ for different β . β is adjusted in a wide range from $\beta = 0$ (linear case) to $\beta = 1.5$ (representing the highly nonlinear case). The number of bin is fixed at $b \equiv (L - 1)/2$ and has been verified to be efficient to derive the space-space correlation information. The size of the ensemble for detecting both correlation functions is about 8×10^9 .

IV. RESULTS

A. Scaling for linear and highly nonlinear cases

We start with studying the following two limiting cases. The first one is the linear system with $\beta = 0$, for which one can use the formula from the theory of phonon random walks [39]

$$\rho_Q(m, t) \simeq \left| \frac{1}{2\pi} \int_{-\pi}^{\pi} e^{i(mq - \omega_q t)} dq \right|^2 \quad (5)$$

to predict $\rho_Q(m, t)$. Inserting the phonon dispersion (2) into formula (5), one then gains the prediction of $\rho_Q(m, t)$, which has been well verified by simulations [39]. The second is the highly nonlinear case. For such system, the nonlinear hydrodynamics theory [13, 14] has predicted the heat mode's correlation function to be the Lévy distribution and satisfying the following scaling property [11, 12]

$$t^{1/\gamma} \rho_Q(m, t) \simeq \rho_Q\left(\frac{m}{t^{1/\gamma}}, t\right) \quad (6)$$

with $\gamma = 3/2$ the predicted scaling exponent. Note that such a prediction of γ value requires the associated po-

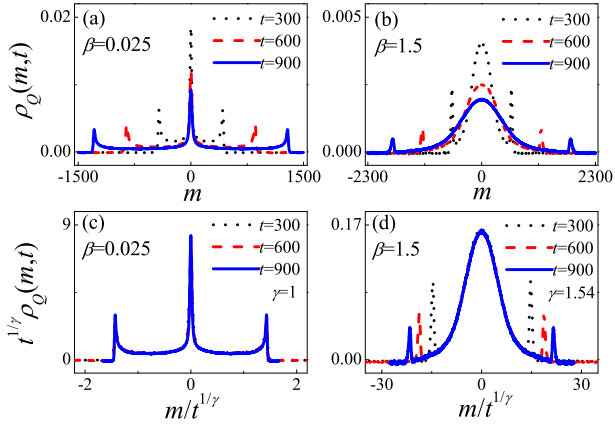


FIG. 2: (a) and (b) Profiles of $\rho_Q(m,t)$; (c) and (d) rescaled $\rho_Q(m,t)$ under formula (6). Here, three long times $t = 300$ (dotted), $t = 600$ (dashed) and $t = 900$ (solid) and two β values $\beta = 0.025$ and $\beta = 1.5$ are considered for comparison.

tential of the system to be symmetric and the internal averaged pressure $\langle F \rangle$ to be zero, our focused system here naturally bears such property.

With such theoretical understanding, now let us turn to the simulation results. Figure 2 presents the profiles of $\rho_Q(m,t)$ and their scaling properties for three typical times and two β values, among which, $\beta = 0.025$ denotes the system close to the linear case; while $\beta = 1.5$ we employ to represent the highly nonlinear case. As expected, on one hand, at the relatively small β value, the profile of $\rho_Q(m,t)$ is mainly dependent on the phonon dispersion relation (2) determined by formula (5) and following the ballistic scaling ($\gamma = 1$) [see Fig. 2(a) and (c)] if compared to the prediction of [39], especially that we see a highly localized peak on the origin ($m = 0$). Such localized peak of $\rho_Q(m,t)$ mainly stems from the special phonon dispersion relation [Eq. (2) and Fig. 1], where as we have already mentioned that, there is a wider q domain with zero group velocities near the Brillouin zone boundary. On the other hand, the situation for the cases of relatively large nonlinearity is quite different: The highly localized central peak now disappears, instead, a common quasi superdiffusive ($\gamma = 1.54$) Lévy walks profile can be observed [see Fig. 2(b) and (d)]. This seems to indicate that the nonlinearity can cause the delocalization of $\rho_Q(m,t)$ in certain domain induced by the phonon dispersion relation. Therefore, it would be interesting to study in more detail of such delocalization process, which may help us to fully understand both roles of phonon dispersion and nonlinearity.

B. Multiscaling in the intermediate range of nonlinearity

Before going on, let us first see some typical profiles of $\rho_Q(m,t)$ in the intermediate range of β values to gain a preliminary impression. Figure 3 presents such a result,

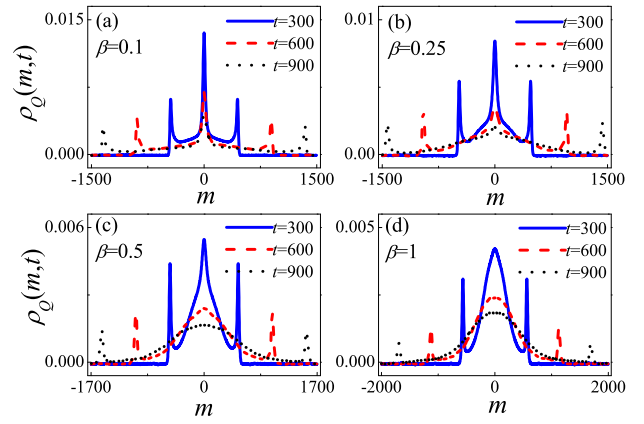


FIG. 3: Profiles of $\rho_Q(m,t)$ for three long times $t = 300$ (solid), $t = 600$ (dashed) and $t = 900$ (dotted) and four β values in the intermediate range: (a) $\beta = 0.1$; (b) $\beta = 0.25$; (c) $\beta = 0.5$ and (d) $\beta = 1$.

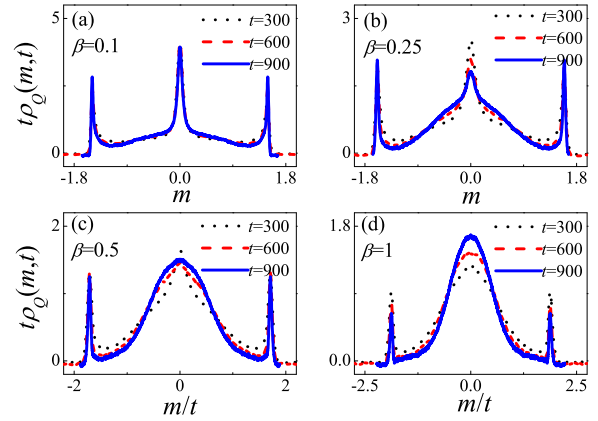


FIG. 4: Rescaled $\rho_Q(m,t)$ according to formula (6) with $\gamma = 1$ for three long times $t = 300$ (dotted), $t = 600$ (dashed) and $t = 900$ (solid) and four β values in the intermediate range: (a) $\beta = 0.1$; (b) $\beta = 0.25$; (c) $\beta = 0.5$ and (d) $\beta = 1$.

from which a detailed crossover from localization to delocalization of the central peak of $\rho_Q(m,t)$ can be clearly identified. Since such an unusual localized shape is exhibited in the center, one can expect that the scaling formula (6) is now no longer valid, but whatever one can first use that scaling formula with $\gamma = 1$ to rescale the profiles to see how the ballistic transport (mainly induced by the phonon dispersion dispersion) can be destroyed by increasing the nonlinearity. For such purpose, in Fig. 4 we plot the result of rescaled $\rho_Q(m,t)$ under ballistic scaling ($\gamma = 1$). As can be seen, with the increase of β , indeed, the distortion of ballistic scaling first originates from the central part and then walks towards the direction of front parts, while it should be noted that if one only looks at the front peaks, the ballistic scaling seems still available. Viewing this fact, it is reasonable to conjecture that $\rho_Q(m,t)$ should at least bears two-scaling behaviors: $\gamma = 1$ for the front peaks and $\gamma \neq 1$ for others. To further

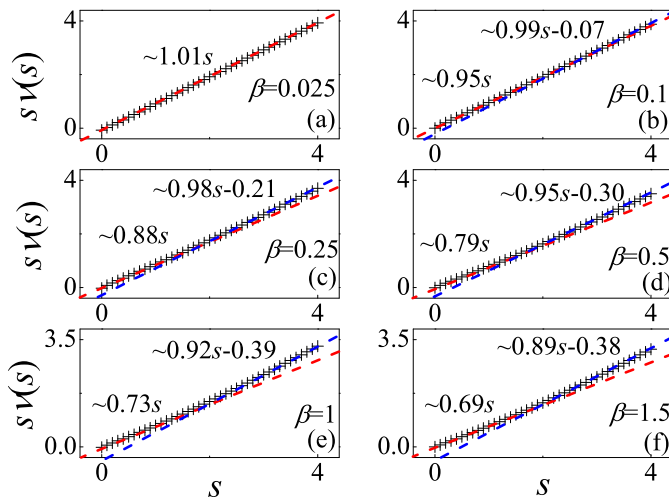


FIG. 5: $s\nu(s)$ vs s for indicating the multiscaling property of $\rho_Q(m, t)$ for (a) $\beta = 0.025$; (b) $\beta = 0.1$; (c) $\beta = 0.25$; (d) $\beta = 0.5$; (e) $\beta = 1$ and (f) $\beta = 1.5$, respectively.

verify this multiscaling property, we here follow [48–50] to study the s ($s > 0$) order momentum of $\rho_Q(m, t)$, i.e., $\langle |m(t)|^s \rangle = \int_{-\infty}^{\infty} |m(t)|^s \rho_Q(m, t) dm$, from which for the strong anomalous diffusion process, $\langle |m(t)|^s \rangle$ has been conjectured to follow $\langle |m(t)|^s \rangle \sim t^{s\nu(s)}$ with $\nu(s)$ to be a s -dependent exponent [50]; while for the ballistic (normal) transport, it is easy to find that $\nu(s)$ will be close to 1 (1/2). Therefore, this s -dependent scaling exponent $s\nu(s)$ is useful to characterize anomalous superdiffusive thermal transport distinct from both ballistic and normal cases.

Figure 5 depicts the results of $s\nu(s)$ versus s calculated from $\rho_Q(m, t)$ for several typical β values, from small to large. As can be seen, with the increase of β , $s\nu(s)$ first shows a single linear scaling with s [see Fig. 5(a)], indicating $\nu(s) \approx 1$ and suggesting the ballistic heat transport; then at about $\beta = 0.1$ this single scaling behavior is destroyed for low order s , eventually, a bilinear scaling behavior starts to appear [see Fig. 5(b)]; finally, for the relatively large β values, we see a scaling exponent for the low order s , denoted by $\nu^L(s)$, close to $\nu^L(s) \approx 0.6$ - 0.7 [see Fig. 5(f)].

It would be worthwhile to note that such particular bilinear scaling behavior has recently been theoretically addressed in the Lévy walks model within the superdiffusive regime [its density follows the scaling formula (6) with $1 < \gamma < 2$], where γ is explained as the power law exponent from the waiting time distribution $\phi(\tau) \sim \tau^{-1-\gamma}$ of the model (see [48, 49] for details). In that Lévy walks model, $\nu^L(s)$ is predicted to be $1/\gamma$ [48, 49]. Therefore, essentially $\nu^L(s)$ involves important information for describing superdiffusive transport. For this reason, we further examine the result of $\nu^L(s)$ versus β in Fig. 6. As can be seen, a detailed crossover from ballistic ($\nu^L(s) = 1$, thus $\gamma = 1$) to superdiffusive ($1/2 < \nu^L(s) < 1$, thus $1 < \gamma < 2$) transport at a critical point of $\beta_c \simeq 0.02$ can be clearly identified. This critical point of β_c is consis-

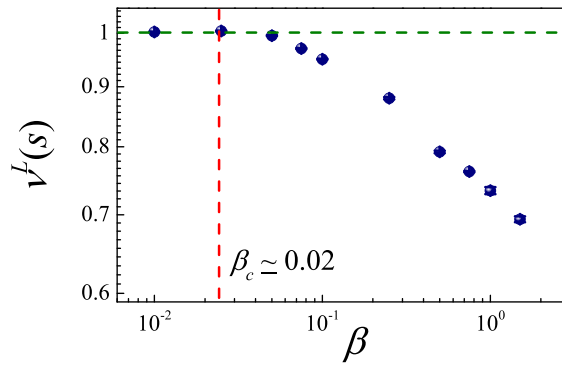


FIG. 6: The fitting values of $\nu^L(s)$ vs β , where the horizontal (vertical) dashed line represents $\nu(s) = 1$ ($\beta_c \simeq 0.02$).

tent with the same value of β_c found in the FPU- β system with NN coupling only [35], where it has been conjectured to be related to the strong stochasticity threshold of the system [51].

For the highly nonlinear case ($\beta = 1.5$ for example), bearing in mind both the predictions of $\nu^L(s) = 1/\gamma$ from the Lévy walks model [48, 49] and $\gamma = 3/2$ from the nonlinear hydrodynamics theory [13, 14], now we make a comparison of our data with the predictions. From Fig. 5(f) we know $\nu^L(s) = 0.69$, hence γ is about 1.45 according to [48, 49]. In view of the measurement errors, this result is consistent with the prediction of $\gamma = 3/2$ [13, 14] and the result of $\gamma = 1.54$ from the scaling analysis as shown in Fig. 2(d).

C. Delocalization of the central peak

After studying the whole scaling property of $\rho_Q(m, t)$, let us consider the delocalization process of the central peak. In fact, since a peculiar phonon dispersion relation is exhibited in the domain near the Brillouin zone boundary (see Fig. 1), it can be expected that the scaling behavior of this central peak is more complicated, based on which the competition between phonon dispersion and nonlinearity can be revealed more detailedly. To further demonstrate this point, we first employ the result of Fig. 2(c) once again, i.e., the rescaled $\rho_Q(m, t)$ under $\beta = 0.025$, to give a more emphasis on the central peak's scaling. As shown in Fig. 7, clearly, although the whole shapes of $\rho_Q(m, t)$ for different t can be nearly perfectly rescaled by ballistic scaling ($\gamma = 1$) [see Fig. 2(c)], the scaling of just this central peak shows some deviations.

Viewing this fact, next we investigate how the decay of this central peak would depend on the nonlinearity. Generally, we find that $\rho_Q(0, t)$ decays with t in a power-law, i.e., $\rho_Q(0, t) \sim t^{-\eta}$ with η a time scaling exponent. Such relevant results for several typical β values are plotted in Fig. 8, among which we note that the result of $\beta = 0$ is derived from the theoretical formula of Eq. (5) suggesting the fact of $\eta = 1/2$ [see Fig. 8(a)]. Interestingly, com-

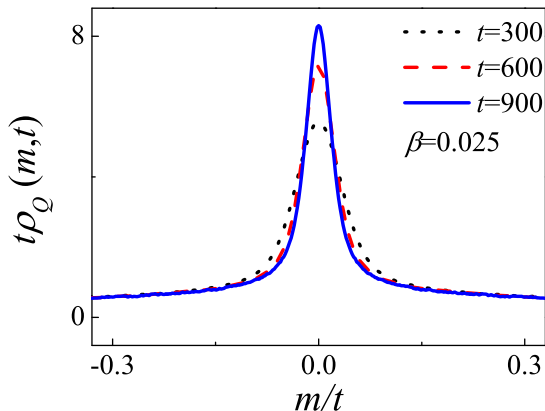


FIG. 7: Rescaled $\rho_Q(m, t)$ under the ballistic scaling ($\gamma = 1$) for $\beta = 0.025$ to indicate that for the central peak, the ballistic scaling is not perfectly valid.

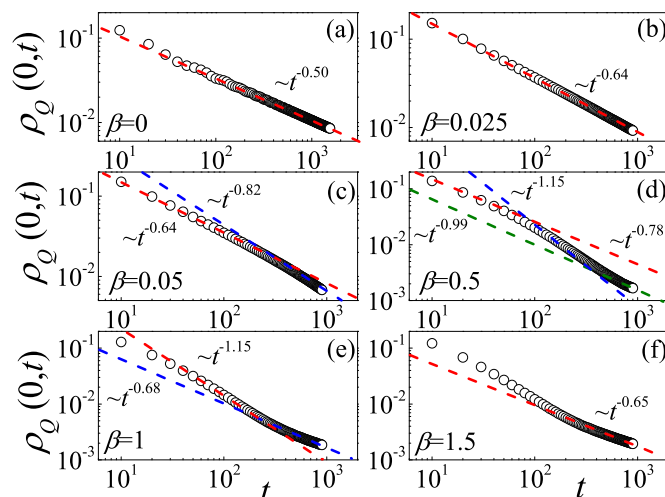


FIG. 8: $\rho_Q(0, t)$ vs t for indicating the scaling property of central peak: (a) $\beta = 0$; (b) $\beta = 0.025$; (c) $\beta = 0.05$; (d) $\beta = 0.5$; (e) $\beta = 1$ and (f) $\beta = 1.5$, respectively.

pared to the whole scaling property of $\rho_Q(m, t)$, Fig. 8 indicates that the picture of the decay of $\rho_Q(0, t)$ for different t is richer, i.e., with the increase of β , $\rho_Q(0, t)$ first decays with one single η value [see Fig. 8(a)-(b)]; then at about $\beta = 0.05$, an additional η value in the range of long t emerges [see Fig. 8(c)]; after that if one increases β further, totally three η values can be observed [see Fig. 8(d)]; while eventually, for the highly nonlinear case, the third scaling exponent in a long time, denoted by η^L , seems dominated [see Fig. 8(f)]. A careful examination of the turning point from one to two-scaling exponents suggests a critical point of $\beta_c \simeq 0.02$, which is similar to that demonstrated in Fig. 6. This implies that the time scaling exponent η of the central peak of $\rho_Q(m, t)$ also involves key information for characterizing anomalous thermal transport.

Finally, as one usually concerns with the long time asymptotic behavior of heat transport property, in Fig. 9

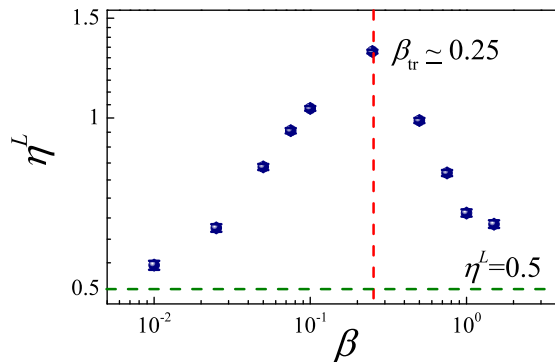


FIG. 9: η^L vs β , where the horizontal (vertical) dashed line denotes $\eta^L = 0.5$ ($\beta_{tr} \simeq 0.25$).

we further plot the result of η^L versus β . One can see that, as β increases from 0.025 to 1.5, η^L increases first, then reaches its maximum value at about $\beta_{tr} \simeq 0.25$, finally decreases down to $\eta^L \approx 3/2$ with the similar value of the scaling exponent γ shown in Fig. 2(d). Obviously, such asymptotic decay behavior of the central peak with β is *nonmonotonic*, which is consistent with the same nonmonotonic variation of the size-dependent scaling exponent of heat conductivity with temperature in the same model [41], thus further supporting the fact that the heat conduction of this system is nonuniversal, dependence of certain system's parameters [41].

V. DISCUSSION

We are particularly interested in the underlying mechanism of the observed nonmonotonic delocalization process of $\rho_Q(m, t)$. From the microscopic point of view, this can be understood by the property of intraband DBs [41], which is nonmonotonically dependent on the temperature, hence it is nonmonotonically dependent on the nonlinearity. Eventually if the heat transport can be understood by the picture of phonons scattered by such intraband DBs, a nonmonotonic delocalization of $\rho_Q(m, t)$ with β could be expected [41]. We here aim to explore this scattering process of phonons from a macroscopic point of view. For this aim, in the following we shall employ the correlation function of momentum perturbations to reveal the information of such scattering process.

The momentum spread described by its perturbations correlation function $\rho_p(m, t)$ contains useful information in understanding heat transport of momentum-conserving systems. As mentioned in Sec. III, $\rho_p(m, t)$ may correspond to the sound modes' correlation in hydrodynamics theory [13, 14, 29]. A diffusive momentum spread has been conjectured to be the origin of the normal heat transport observed in coupled rotator systems [52]. This nonballistic spread of momentum has also been revealed in another special system with

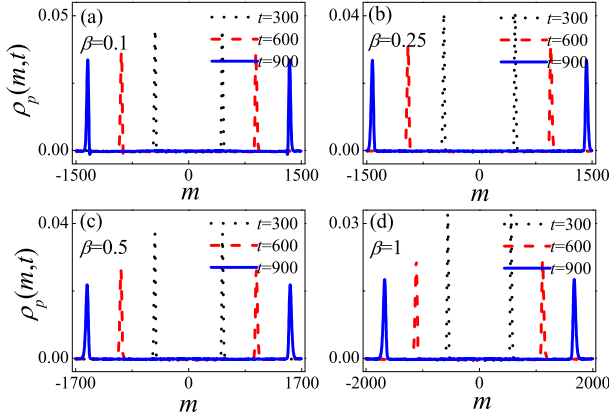


FIG. 10: Profiles of $\rho_p(m, t)$ for three long times $t = 300$ (dotted), $t = 600$ (dashed) and $t = 900$ (solid) and four β values in the intermediate range: (a) $\beta = 0.1$; (b) $\beta = 0.25$; (c) $\beta = 0.5$ and (d) $\beta = 1$.

a double-well interparticle potential [36]. In the phonon random walks theory, the momentum correlation function in linear systems has been proved to be a quantum like wave function's real part, while this quantum wave function itself modulus square can represent the heat perturbations correlation function [39]. A more recent work [53] developed an effective linear stochastic structure theory to derive the momentum spreading correlation function in the long time limit, and demonstrated that anomalous thermal transport is dominated by the longwavelength renormalized waves [54–56].

We begin with presenting some typical results of $\rho_p(m, t)$ in Fig. 10. Here, three long times and four β values the same as those in Fig. 3 are considered. As can be seen, all the profiles of $\rho_p(m, t)$ suggest nondiffusive ballistic behaviors, which are the evidences of anomalous heat transport. In particular, three points can be revealed: First, the moving velocities of the front peaks are increased with the increase of β , which is a natural property of the systems with hard-type anharmonicity [37], and can be understood from the renormalized waves theory [54–56]. Second, as β increases, a slight broadening of the side peaks can be identified. This broadening is related to the sound attenuation [29]. In the hydrodynamic theory [4, 5, 7–10, 13, 14], it has been usually suggested that there is a mode-dependent damping coefficient $\Gamma_q \sim D|q|^\delta$ in the small wavenumbers limit, where D is a damping constant and δ is a scaling exponent. Then, the constant D can be inferred from this broadening [53].

Finally, for each β value, the front peaks of $\rho_p(m, t)$ decay with t in a power law: $h \sim t^{-\delta}$, here h is the height of the peaks. This power-law exponent δ has been conjectured to correspond to the exponent shown in Γ_q [53]. It may also correspond to both the scaling exponents of sound modes' correlation function predicted by the nonlinear hydrodynamics theory [13, 14] and of the heat current power spectra suggested by the mode coupling [4, 5]

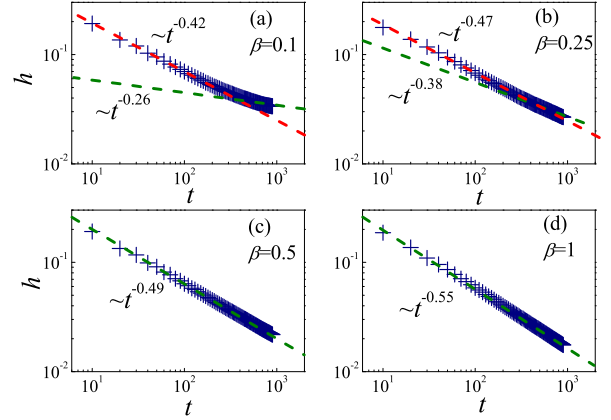


FIG. 11: The height h of the front peaks of $\rho_p(m, t)$ decays with t : (a) $\beta = 0.1$; (b) $\beta = 0.25$; (c) $\beta = 0.5$ and (d) $\beta = 1$.

or mode cascade [7–10] theory. For this reason, we here examine detailedly the decay of this ballistic front peak of $\rho_p(m, t)$ in some intermediate ranges of β values (see Fig. 11). Remarkably, we find that this decay behavior also shows a sensitive dependence of β . In particular, around a turning point of $\beta_{tr} \simeq 0.25$, there is a crossover from two-scaling exponents (for small β) to one-scaling (for large β). Eventually, for the relatively large β values, the values of δ seem to converge to a value of 0.5–0.6 [see Fig. 11(c) and (d)], which is almost consistent with the value of $\delta = 1/2$ predicted by the relevant theories in the long time limit [4, 5, 7–10, 13, 14]. However, for the relatively small β values in this intermediate range, obviously, it seems to show some deviations.

Given the same turning point of $\beta_{tr} = 0.25$, it is reasonable to conjecture that there should be a close relationship between the delocalization of the central peak of $\rho_Q(m, t)$ and the decay of the side peaks of $\rho_p(m, t)$. Such a relation revealed here is amazing, since the central peak of $\rho_Q(m, t)$ is contributed by phonons with high wave numbers, while the side peaks of $\rho_p(m, t)$ are represented by those with low q , in view of their different group velocities. So, even that there are some couplings between $\rho_Q(m, t)$ and $\rho_p(m, t)$, such couplings should naturally arise at the same locations with the same q (the same group velocities) [34]. However, our results here seem to violate this natural intuition.

Turning back to the related theoretical models, the nonlinear hydrodynamics theory [13, 14] claimed that, for sound modes, the correction from the coupling of heat mode will vanish in the long time limit, but it decays very slowly, so at the intermediate time scales, one could see some physically interesting information of the heat and the sound modes' coupling. But obviously, the nonlinear hydrodynamics theory did not tell us that the coupling between the sound and the heat modes' correlation can be so unusual. As to this point, we note that the assumption of the mode cascade theory [7–10] may present a correct picture. The central argument the authors suggested is that, the thermal conductivity at any

(sufficiently low) frequency can be entirely determined by the thermal conductivity and bulk viscosity (represented by the momentum transport) at much higher frequency. This sort of unusual coupling between the heat transport and the momentum transport, which is the explicit basis of the mode cascade theory [7–10], seems to be supported by our present results here, although the argument is still hard to examine in more detail.

VI. CONCLUSION

To summarize: We have employed the heat perturbation correlation function $\rho_Q(m, t)$ to investigate anomalous thermal transport in a 1D FPU- β lattice including both the NN and NNN interactions. After choosing an appropriate coupling ratio, we have obtained a peculiar phonon dispersion relation which then enables us to examine both roles of phonon dispersion and nonlinearity in more detail. It has been found that, for relatively small and large nonlinearity, the transport are ballistic and Lévy walks types, respectively, which can be well understood from the predictions of the concept of phonon random walks [39] and the theory of nonlinear fluctuating hydrodynamics [13, 14]. While more interesting things take place in the intermediate range of the nonlinearity, where we emphasize that, there both the phonon dispersion relation and nonlinearity can play the roles. In this intermediate range, we have found that: (i) there is a transition from the single scaling to multiscaling for the whole profiles of $\rho_Q(m, t)$ with a critical point of $\beta_c \simeq 0.02$; (ii) the delocalization of the central peak of $\rho_Q(m, t)$ shows a *nonmonotonic* dependence of nonlinearity with another turning point of $\beta_{tr} \simeq 0.25$.

The first critical point of $\beta_c \simeq 0.02$ indicates a crossover from ballistic to nonballistic transport and might be related to the strong stochasticity threshold of the focused FPU- β systems, either or not yet including the NNN interactions [35]. The second turning point of $\beta_{tr} \simeq 0.25$ is a special feature of such systems and seems to be related to the nonuniversal heat conduction observed previously in the same system [41]. In those previ-

ous publications [41], we have conjectured that the microscopic underlying mechanism is caused by the scattering of phonons by intraband DBs. Here instead, we use the momentum perturbation correlation function $\rho_p(m, t)$ to explore this phonons' scattering process from a macroscopic point of view, which makes this conjecture more convincing. Remarkably, we find that the time decay behavior of the side peaks of $\rho_p(m, t)$ follows a similar nonmonotonic β -dependent manner as those shown in $\rho_Q(m, t)$.

Finally, we would like to point out that such a coincidence of the properties of $\rho_Q(m, t)$ and $\rho_p(m, t)$ suggests the very slowly decoupling process of the heat and the sound modes' correlations claimed by nonlinear hydrodynamics theory [13, 14], in particular for the cases in the intermediate range of the nonlinearity (or at the intermediate time scales). It also supports the assumption of the mode cascade theory proposed by G. R. Lee-Dadswell *et al* [7–10], i.e., the unusual coupling between the heat transport and the momentum transport should be taken into account. This is because the heat mode and the sound modes are naturally considered as contributed by the relatively high and low wave-number phonon modes with the relatively high and low frequencies, respectively.

In short, the results presented here might provide further useful information for our understanding of anomalous heat transport and its coupling to the momentum transport, particularly from the perspective of phonon dispersion relation and nonlinearity, though understanding the detailed underlying mechanism still requires efforts.

Acknowledgments

This work was supported by the National Natural Science Foundation of China (Grant No. 11575046); the Natural Science Foundation of Fujian Province, China (Grant No. 2017J06002); the Training Plan Fund for Distinguished Young Researchers from Department of Education, Fujian Province, China, and the Qishan Scholar Research Fund of Fuzhou University, China.

-
- [1] S. Lepri, R. Livi, and A. Politi, *Phys. Rep.* **377**, 1 (2003).
 - [2] A. Dhar, *Adv. Phys.* **57**, 457 (2008).
 - [3] S. Lepri, R. Livi, and A. Politi, *Thermal Transport in Low Dimensions*, Lecture Notes in Physics Vol. 921 (Springer, Berlin, 2016).
 - [4] L. Delfini, S. Lepri, R. Livi, and A. Politi, *Phys. Rev. E* **73**, 060201 (2006).
 - [5] L. Delfini, S. Lepri, R. Livi, and A. Politi, *J. Stat. Mech.* P02007 (2007).
 - [6] O. Narayan and S. Ramaswamy, *Phys. Rev. Lett.* **89** 200601 (2002).
 - [7] G. R. Lee-Dadswell, B. G. Nickel, and C. G. Gray, *Phys. Rev. E* **72**, 031202 (2005).
 - [8] G. R. Lee-Dadswell, B. G. Nickel, and C. G. Gray, *J. Stat. Phys.* **132**, 1 (2008).
 - [9] G. R. Lee-Dadswell, *Phys. Rev. E* **91**, 032102 (2015).
 - [10] G. R. Lee-Dadswell, *Phys. Rev. E* **91**, 012138 (2015).
 - [11] V. Zaburdaev, S. Denisov, and J. Klafter, *Rev. Mod. Phys.* **87**, 483 (2015).
 - [12] V. Zaburdaev, S. Denisov, and P. Hänggi *Phys. Rev. Lett.* **106**, 180601 (2011).
 - [13] C. B. Mendl and H. Spohn, *Phys. Rev. Lett.* **111**, 230601 (2013).
 - [14] H. Spohn, *J. Stat. Phys.* **154**, 1191 (2014).
 - [15] S. Lepri, R. Livi, and A. Politi, *Phys. Rev. Lett.* **78**, 1896 (1997).

- [16] A. Dhar, Phys. Rev. Lett. **88**, 249401 (2002).
- [17] P. Grassberger, W. Nadler, and L. Yang, Phys. Rev. Lett. **89**, 180601 (2002).
- [18] G. Casati and T. Prosen, Phys. Rev. E **67**, 015203 (2003).
- [19] T. Mai, A. Dhar, and O. Narayan, Phys. Rev. Lett. **98**, 184301 (2007).
- [20] R. Kubo, M. Toda, and N. Hashitsume, *Statistical Physics II: Nonequilibrium Statistical Mechanics* (Springer, New York, 1991).
- [21] D. Andrieux and P. Gaspard, J. Stat. Mech. P02006 (2007).
- [22] S. Chen, Y. Zhang, J. Wang, and H. Zhao, Phys. Rev. E **89**, 022111 (2014).
- [23] E. Helfand, Phys. Rev. **119**, 1 (1960).
- [24] A. Torcini, P. Grassberger, and A. Politi, J. Phys. A **28**, 4533 (1995).
- [25] G. Giacomelli, R. Hegger, A. Politi, and M. Vassalli, Phys. Rev. Lett. **85**, 3616 (2000).
- [26] C. Primo, I. G. Szendro, M. A. Rodriguez, and J. M. Gutiérrez, Phys. Rev. Lett. **98**, 108501 (2007).
- [27] H. Zhao, Phys. Rev. Lett. **96**, 140602 (2006).
- [28] N. Li, B. Li, and S. Flach, Phys. Rev. Lett. **105**, 054102 (2010).
- [29] S. Chen, Y. Zhang, J. Wang, and H. Zhao, Phys. Rev. E **87**, 032153 (2013).
- [30] S. G. Das, A. Dhar, K. Saito, C. B. Mendl, and H. Spohn, Phys. Rev. E **90**, 012124 (2014).
- [31] S. Liu, P. Hänggi, N. Li, J. Ren, and B. Li Phys. Rev. Lett. **112**, 040601 (2014).
- [32] J. Wang, D. He, Y. Zhang, J. Wang, and H. Zhao, Phys. Rev. E **92**, 032138 (2015).
- [33] J. Wang, Y. Zhang, and H. Zhao, Phys. Rev. E **93**, 032144 (2016).
- [34] A. Kundu and A. Dhar, Phys. Rev. E **94**, 062130 (2016).
- [35] D. Xiong, Europhys. Lett. **113**, 140002 (2016).
- [36] D. Xiong, J. Stat. Mech.: Exp. Theor. (2016) 043208.
- [37] D. Xiong, Phys. Rev. E **95**, 042127 (2017).
- [38] M. Kardar, G. Parisi, and Y. C. Zhang, Phys. Rev. Lett. **56** 889 (1986).
- [39] D. Xiong and E. Barkai, arXiv:1606.04602v4 (2016).
- [40] Z. Rieder, J. L. Lebowitz, and E. Lieb, J. Math. Phys. **8**, 1073 (1976).
- [41] D. Xiong, J. Wang, Y. Zhang, and H. Zhao, Phys. Rev. E **85**, 020102 (2012); D. Xiong, Y. Zhang, and H. Zhao, *ibid.* **90**, 022117 (2014).
- [42] S. V. Dmitriev, A. P. Chetverikov, and M. G. Velarde, Phys. Status. Solidi B **252**, 1682 (2015).
- [43] D. Bagchi, Phys. Rev. E **95**, 032102 (2017).
- [44] M. Romero-Bastida, J. O. Miranda-Peña, and J. M. López, Phys. Rev. E **95**, 032146 (2017).
- [45] P. Hwang and H. Zhao, arXiv:1106.2866v1 (2011).
- [46] D. Forster, *Hydrodynamic Fluctuations, Broken Symmetry, and Correlation Functions* (Benjamin, New York, 1975).
- [47] J. P. Hansen and I. R. McDonald, *Theory of Simple Liquids*, 3rd ed. (Academic, London, 2006).
- [48] A. Rebenshtok, S. Denisov, P. Hänggi, and E. Barkai, Phys. Rev. Lett. **112**, 110601 (2014).
- [49] A. Rebenshtok, S. Denisov, P. Hänggi, and E. Barkai, Phys. Rev. E **90**, 062135 (2014).
- [50] P. Castiglione, A. Mazzino, P. Muratore-Ginanneschi, and A. Vulpiani, Physica D (Amsterdam) **134**, 75 (1999).
- [51] S. Lepri, R. Livi, and A. Politi, *Anomalous heat conduction*, a chapter of the book “Anomalous transport: foundations and applications” edited by R. Klages, G. Radons, and I. M. Sokolov.
- [52] Y. Li, S. Liu, N. Li, P. Hänggi, and B. Li, New J. Phys. **17**, 043064 (2015).
- [53] Shi-xiao W. Jiang, H. H. Lu, D. Zhou, and D. Cai, New J. Phys. **18**, 083028 (2016).
- [54] B. Gershgorin, Y. V. Lvov, and D. Cai, Phys. Rev. Lett. **95**, 264302 (2005).
- [55] B. Gershgorin, Y. V. Lvov, and D. Cai, Phys. Rev. E **75**, 046603 (2007).
- [56] Shi-xiao W. Jiang, H. H. Lu, D. Zhou, and D. Cai, Phys. Rev. E **90**, 032925 (2014).